Engineering Notes

Optimization of Dielectric Barrier Discharge Plasma Actuators for Icing Control

Haiyang Hu,* Xuanshi Meng,† and Jinsheng Cai‡
*Northwestern Polytechnical University, 710072 Xi'an,
People's Republic of China*
Wenwu Zhou§
*Shanghai Jiao Tong University, 200240 Shanghai,
People's Republic of China*
Yang Liu¶
East Carolina University, Greenville, North Carolina 27858
and
Hui Hu**
Iowa State University, Ames, Iowa 50011

Nomenclature

c	=	chord length of airfoil, m
Re	=	chord Reynolds number without water spray
T	=	surface temperature, °C
T_∞	=	static temperature of air, °C
t	=	time, s

I. Introduction

ICING is regarded as a severe safety issue for the industry, such as aviation and wind energy in cold weather, because it will degrade the performance when supercooled water droplets impinge and freeze onto the surface of the airfoil and rotating blades. The contamination of the streamlined profile will cause serious degradation of the aerodynamic efficiency and unbalance the whole rotor system. Therefore numerous studies have focused on this icing phenomenon and various anti-/de-icing technologies have been developed in the past few decades [1–5]. However, the current anti/de-icing technology is not sufficient to address the ever-evolving requirements in aerodynamics, materials and energy consumption [6]. As a result, the novel methods and techniques for extended durability and efficient anti-/deicing performance are considered desirable [7–13].

Plasma flow control has received growing research attention in the past few decades for its unique features, such as no moving parts, fast response, and exceptional ease of installation on the surface without changing the shape. One such significant development is the use of surface dielectric barrier discharge (SDBD) plasma actuators, which are composed of two electrodes separated by a dielectric material arranged in an asymmetric fashion [14–17]. The most common SDBD plasma flow control methods include alternative-current surface-dielectric-barrier-discharge (AC-SDBD) and nanosecond-pulse surface-dielectric-barrier-discharge (NS-SDBD) plasma actuations.

The mechanism of AC-SDBD plasma flow control has been studied by different researchers in recent years [14,16]. The results for different researchers are consistent, i.e., application of a sufficiently high-voltage ac signal between the electrodes weakly ionizes the air over the dielectric covering the encapsulated electrode. The ionization of the air is a dynamic process within the ac cycle. The ionized air, in the presence of the electric field, results in a body force vector. Such induced airflow can impart momentum to the flow, just like flow suction or blowing, but without mass injection.

For the NS-SDBD plasma actuator, it has great potential in high-speed flow control; however, its different aerodynamic effects at different timescales make its mechanism in the flow control much more complicated. In addition, because the input is a high-voltage signal of the nanosecond level, its electromagnetic interference is much stronger than that of the AC-SBDB, causing serious interference to the control and measurement equipment of the icing wind tunnel.

Recently, researchers have achieved effective flow control results at higher wind speeds and Reynolds numbers through the optimization of the actuator geometry, substrate materials, and other parameters [18–20]. Using AC-SDBD plasma actuation, Zhang et al. [19] showed the effective flow control over an airfoil with an inflow velocity of 100 m/s using a symmetrically arranged encapsulated electrodes actuator; Kelley et al. [18] achieved effective flow control with an inflow velocity at a $Ma = 0.4$ and a Reynolds number of 2.3×10^6 using 3.175-mm-thick ceramics as the insulating materials. Using NS-SDBD plasma actuation, Nishihara et al. [20] demonstrated effective bow shock perturbations with an incoming flow Mach number of five.

However, the drawback of plasma flow control is its low efficiency of energy conversion (the surface discharge-induced kinetic efficiency versus the discharge current is only several percent) [14]. The part of the electrical energy which is converted to heat remains useless as far as flow control applications are concerned [21–24].

Meng et al. [25,26] and Cai et al. [27] proposed a research method for icing control using AC-SDBD plasma actuation, which can make full use of the aerodynamic and thermal effects of SDBD plasma discharge. Meng et al. [26] and Cai et al. [27] showed the feasibility of SDBD plasma icing control on a cylinder model. The anti-/deicing performance of the AC-SDBD plasma actuator was evaluated based on visualization and thermal images in an icing wind tunnel.

Compared with the traditional anti-/de-icing system, AC-SDBD plasma almost satisfies all the icing control requirements of the next-generation aircraft design. First it can be flush mounted on the surfaces without interfering with the flow to keep the natural laminar flow, and it can be used for flow control when the aircraft is not in the icing condition during flight. Second, it can fully use the discharge energy of the AC-SDBD, i.e., both the thermal and aerodynamic effects. Besides, the self limiting nature of the discharge limits the rise in temperature of the AC-SDBD plasma thereby protecting the composite structures from over-heating during anti-/deicing. Lastly, with the development of the model battery technology, the AC-SDBD actuator can be powered by battery-driven pocket high-voltage generators, which have been installed on unmanned aerial vehicles in several field tests as electronic rudders [28]. Therefore, the AC-SDBD actuators can be comfortably mounted on an all-electric aircraft as a full electric-based icing control technique.

*Graduate Student; currenty Doctorate, Iowa State University, Iowa 50011.
†Professor; mxsbear@nwpu.edu.cn (Corresponding Author).
‡Professor; jcai@nwpu.edu.cn.
§Assistant Professor; zhouww@sjtu.edu.cn.
¶Assistant Professor; liuya19@ecu.edu.
**Professor; huhui@iastate.edu.

Inspired by the aforementioned advantages, the plasma icing control studies are experiencing rapid development. Zhou et al. [29] conducted the study over an airfoil model using SDBD plasma generation for icing mitigation. The results demonstrated that SDBD plasma actuators could be used as a promising anti-icing tool for aircraft by taking advantage of the thermal effects associated with plasma generation. Tian et al. [30] showed an effective icing control using a pulsed dielectric barrier discharge plasma actuation with a freestream velocity of 90 m/s, which exhibited the compatibility of SDBD plasma actuation in preventing aircraft icing in flight for real applications. Liu et al. [31] revealed that the AC-SDBD plasma actuators have a great potential for more efficient anti-/deicing operations on aircraft in comparison with the conventional electrothermal methods.

Furthermore, Meng et al.'s [32] research showed that the coupling between plasma-induced flow and thermal effects of the discharge form the fundamental mechanism for the icing control of AC-SDBD plasma actuation. For optimization of the actuators, both the discharge heat and the induced aerodynamic effects of the plasma actuation must be considered.

In most icing control studies, the design and placement of the actuator are directly used as the parameters in the flow control studies; i.e., the actuators were attached mostly around a separation point on the upper surface of the airfoil [14]. As a result, the optimization of an AC-SDBD plasma actuator for the anti-/de-icing study is necessary. In the present research, both the original design of the plasma actuator based on flow control and the optimized design of the actuator for anti-icing are validated experimentally on a realistic configuration of the NACA0012 airfoil model. The criterion for actuator optimization is to elevate the ability of anti-icing, i.e., to ensure that most of the airfoil is free of ice accretion. The surface temperature distribution and ice accretion images are used to observe the anti-icing effects in detail.

II.   Experiment Setup

The anti-icing experiments were conducted in a closed-circuit low-speed icing research wind tunnel at the Aerospace Engineering Department of Iowa State University. The test section is 2.0 m long that is 0.4 m (height) $\times$ 0.4 m (width) in cross section.

All four sidewalls were made transparent to have optical access for the high-speed camera as well as Infra Red camera. The NACA0012 airfoil was chosen as the test model. The chord length of the airfoil was set at 0.15 m, and the spanwise distance was 0.4 m. The angle of attack was fixed at $-5°C$ for all the test cases. Only the icing control over the leading edge and the upper surface was studied due to less ice accumulation over the lower surface and the limitation of the experimental setup.

In the present study, the freestream velocity was kept constant at $U_\infty = 40$ m/s, and the surrounding air temperature was $T_\infty = -10°C$. The corresponding Reynolds number Re number was about 3.6×10^5 based on the chord of the airfoil in the airflow without water spray. The liquid water content (LWC) of the incoming airflow was 1.0 g/m³. For all the test cases, the icing wind tunnel was operated at a prescribed temperature level for about 20 min to ensure the test section reached the thermal equilibrium. Then, the SDBD plasma actuator was switched on for about 10 s before turning on the water spray system. The origin of the time was set at the beginning of the water spray. As the water spray system was switched on, the super-cooled water droplets carried by the incoming airflow would impinge onto the surface of the airfoil model.

A multi-SDBD plasma actuator (i.e., actuator consisting of several long single stripe actuators) was installed on the surface of the airfoil. The single SDBD actuator was composed of two 0.07-mm-thick copper electrodes, which were arranged asymmetrically. Three layers of Kapton tape (0.056 mm per layer) separated the two electrodes as the dielectric barrier layer; see Fig. 1a. There was no gap or overlap between the exposed and encapsulated electrodes to encourage uniform plasma generation. As shown in Fig. 1b, two sets of multi-SDBD plasma actuators were embedded on the upper surface of the airfoil, symmetrically, to the middle span of the airfoil model.
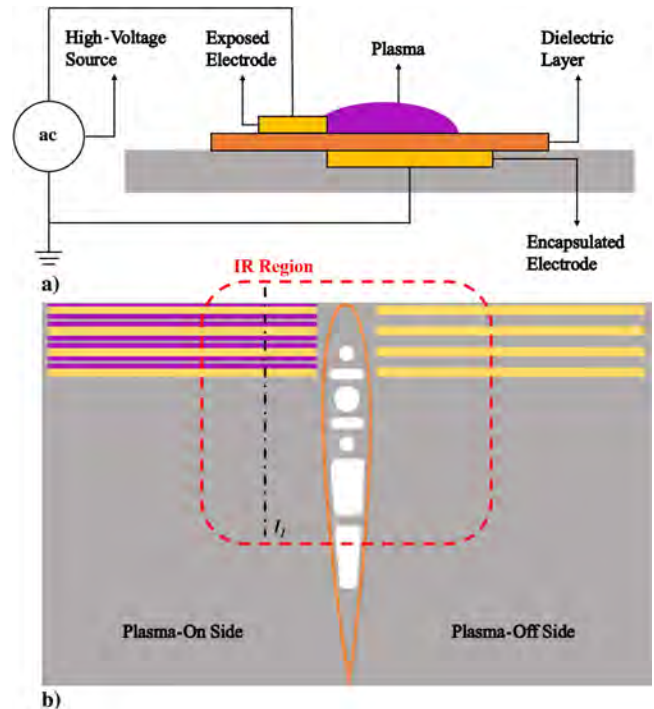

Fig. 1   Schematic illustrations of a) single SDBD plasma actuator design and b) plasma actuators mounted on the upper surface of the airfoil model.

For the single AC-SDBD plasma actuator, a near-wall jet toward the encapsulated electrode is generated. As shown in previous results [32], the induced airflow in this study is perpendicular to the surface of the model due to the interaction of the airflow generated by the adjacent actuators. Such normal flow would enhance the mixing effect between the thermal energy produced by plasma and the cold boundary layer, which will enhance the anti-/deicing efficiency.

During the icing experiment, the starboard-side actuator was always kept off, whereas the portside actuator was turned on for icing control. The anti-icing performance over the airfoil surface for the plasma-on side (i.e., port side) would be compared side by side against that on the plasma-off side (i.e., starboard side) to evaluate the effectiveness of the SDBD plasma actuator under identical icing conditions.

During the experiment, two different actuator configurations (original and optimized) were tested, see Fig. 2. In the case of original actuators inspired by the flow control application, the whole actuator only covered the upper surface and was located around the separation point at the stall angle of attack [33–35].

For the optimized configuration, the difference in comparison with the original one was that the leading edge of the airfoil was covered. The purpose of the optimization was to achieve as much heat accumulation as possible on the leading edge due to the locally low flow speed around the stagnation point. This accumulation of the heat as well as the transfer of it downstream with the incoming flow and the plasma-induced flow are very important for the anti-icing of the airfoil. Moreover, it will ensure less ice accretion probability on the airfoil surface.

The actuator was connected to a high-voltage ac source that could provide a peak-to-peak amplitude varying from 0 to 30 kV and center frequency from 5 to 15 kHz. The voltage applied to the actuator was measured by a Tektronix P6015A high-voltage probe. In this study, the voltage on the actuator was kept at 13 kV and the frequency was set at 10 kHz.

A high-speed imaging system, which was a Dimax model of PCO-Tech, Inc., with a 2000×2000 pixel maximum spatial resolution, along with a 60 mm optical lens (Nikon, 60 mm Nikkor 2.8D) was used to record the ice accretion process. An infrared thermal imaging system (model FLIR-A615) was used to map the corresponding temperature distributions (from the leading edge up to 70 % of chord length) over the surface of the airfoil model during the ice accretion
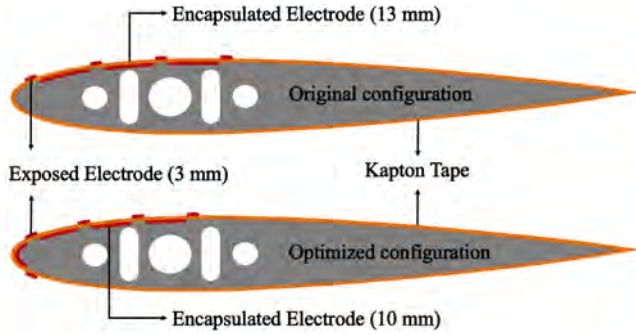
Fig. 2 Schematic illustrations of original and optimized actuators.

process simultaneously. To compare the thermal behavior for two configurations, a reference line ($l1$, illustrated in Fig. 1b) is selected on the plasma-on side of the airfoil to map the temperature distribution.

III. Results

Figure 3 shows the snapshots of the instantaneous images extracted from the high-speed camera results for two different configurations and

the plasma-off side at $t = 143$ s when the heat of the plasma discharge reached a balanced state. Figure 4 exhibits the corresponding surface temperature distributions recorded simultaneously using the IR camera. Figure 5 illustrates the extracted profiles of surface temperature for sample lines l_1.

For the plasma-off side of the airfoil, as demonstrated in Fig. 3c, the evident ice accretion on the airfoil surface is observed, which would cause a lift reduction and drag increment due to the contamination of the streamlined profile over the airfoil.

Figure 3a clearly illustrates the presence of the uniform ice at the leading edge and the fingerlike rivulet structures of ice accretion downstream of the actuator for the plasma-on side for the original design. Figure 4a shows the corresponding upper surface temperature distribution, which confirms the ice accretion in the same area. Figure 5 shows the corresponding surface temperature at l_1. It shows that the temperature corresponding to the icing (i.e., the "frozen temperature") in the present test is about $-3°C$ due to the presence of incoming flow and the water film.

The reason for the fingerlike rivulet structures of ice accretion is that, in the presence of incoming flow, the temperature of the plasma discharge is within $30°C$ [32]; the supercooled droplets cannot be vaporized at that low temperature. But, the supercooled water droplet would be efficiently heated and kept at the liquid state, and it would
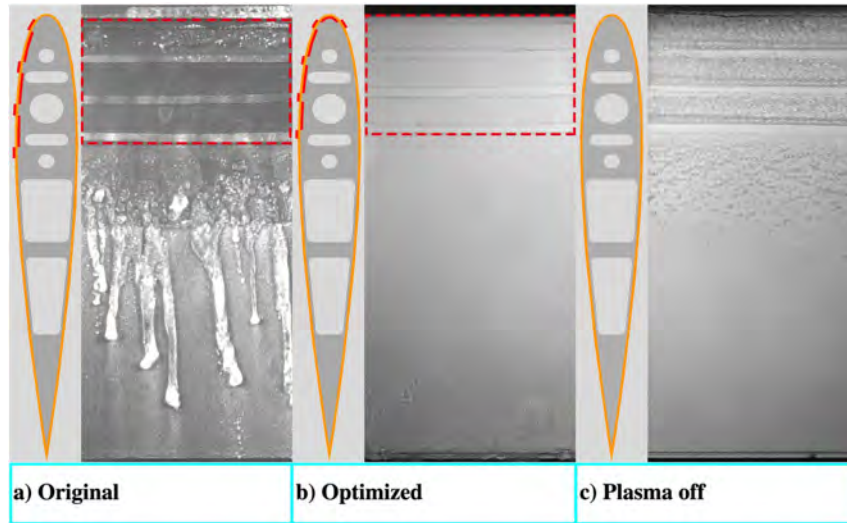

Fig. 3 Ice accretion snapshot over airfoil for different actuators and the plasma-off side for $t = 143$ s, $U_\infty = 40$ m/s, $T_\infty = -10°C$, and LWC = 1.0 g/m³.
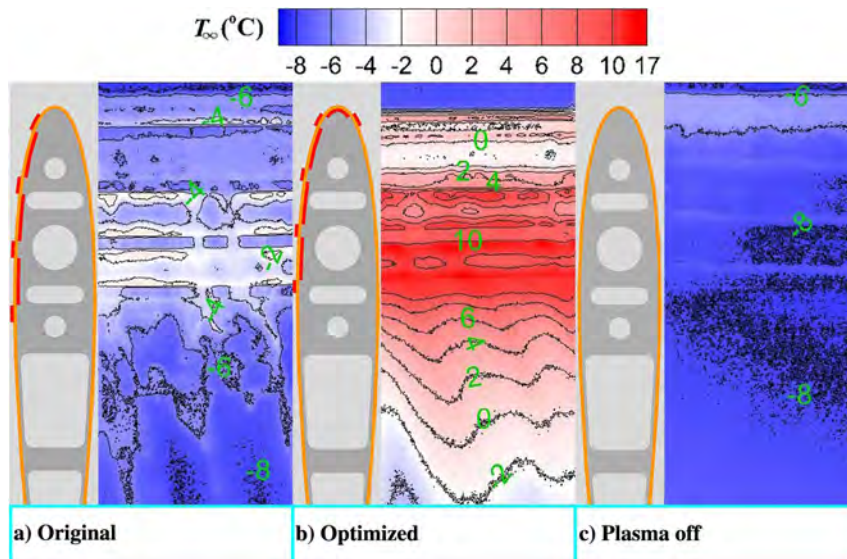

Fig. 4 Infrared images of ice accretion over airfoil for different actuator configurations and the plasma-off side for $t = 143$ s, $U_\infty = 40$ m/s, $T_\infty = -10°C$, and LWC = 1.0 g/m³.

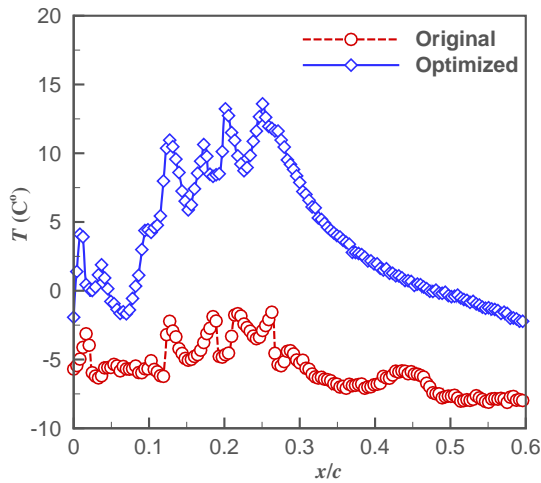**Fig. 5 Infrared images of ice accretion over airfoil for different actuators and the plasma-off side for $t = 143\,\text{s}$, $U_\infty = 40\,\text{m/s}$, $T_\infty = -10°\text{C}$, and $\text{LWC} = 1.0\,\text{g/m}^3$.**

form a thin water film while impinging onto the actuator area due to the thermal effect of the plasma actuator.

For the original design, the heat generated by the plasma is enough to avoid ice accretion on the actuator surface. However, the heat transferred by incoming and plasma-induced flow failed to keep the water film free of ice over the entire airfoil; as a result fingerlike ice accretion was formed. The region of ice accumulation is about $0.6c$ from the leading edge. As demonstrated in Fig. 4a, the thermal effect increased the surface temperature in the actuator region, and the temperature near the edge of the exposed electrodes has risen above the frozen temperature. Also, the leading edge would probably result in a flow separation in the downstream area. This kind of separation would decrease the boundary-layer flow velocity, which drives the runback water passing the airfoil surface. Compared with the streamlined surface, the runback water would be more difficult to drive away by the slower boundary-layer flow in the separation area. Such a condition would lead to more water remaining and freezing on the airfoil surface.

For the plasma-on side of the optimized actuator (see Fig. 4b), there is no ice accumulation on the leading edge; a little ice accumulation occurs on the trailing edge, and the region of it is about $0.1c$ from the trailing edge. It demonstrates that the optimized design of the actuator configuration is more effective for anti-icing in comparison with the original design.

Figure 4b demonstrates the local surface temperature of the optimized actuator. It can be observed that the surface temperature is significantly higher than that of the original (more than two times). Almost all areas of the IR measurements for the optimized actuator are above the frozen temperature; it is as high as 15°C in some regions, which can be seen in Fig. 5.

Figure 3b shows that there is no ice accretion on the leading edge for the optimized design, with minor ice accretion observed on the rear of the airfoil surface, which is due to the accumulation of water at the step of the trailing edge. Figure 5 shows the surface temperature distribution for the original design is below 0°C over the entire surface of the airfoil. However, for the optimized design, 50% of the airfoil surface is above 0°C; and it is much higher than 10°C in some regions.

For the optimized actuator, (i.e., the plasma actuator wrapped around the leading edge;) the plasma induced thermal energy concentrated at the stagnation point was transferred downstream over the surface of the airfoil under the influence of plasma induced flow as well as the oncoming flow. Thus, the optimized actuator avoided the ice accretion that was present in the original configuration and ensured that most of the airfoil was free of the ice accretion. Moreover, the optimized actuator could generate more heat to be converted from the leading edge by the incoming flow, and it could further increase the heating efficiency of downstream actuators.

IV. Conclusions

The experimental results showed that the AC-SDBD plasma actuation anti-icing technology is different from the traditional hot air anti-icing technology. Its heat does not directly vaporize the supercooled water droplets but produces the coupling effect of discharge heat and induced airflow, which retains the supercooled water droplets in liquid state without letting them to freeze into ice. In this case, there is a direct relationship between the placement of the plasma actuators and the aerodynamic characteristics of the airfoil.

Compared with flow control, which focuses on the flow structure manipulation, the purpose of the actuator applied in this study was to keep the airfoil surface free of ice accretion; most important, there should be no ice accretion on the key aerodynamic part, i.e., the leading edge of the airfoil. As proved in the original plasma actuator, the shortage of the leading-edge actuator would cause ice accretion over the leading edge. Moreover, it would weaken the heat transfer efficiency of the actuator without the leading-edge heating. For the optimized actuator, (i.e., the plasma actuator wrapped around the leading edge;) the thermal energy deposited at the stagnation point was transferred further downstream over the surface of the airfoil by the plasma induced flow and oncoming free stream flow. The thermal energy transferred in this case was found to be more than the original actuator and this ensured that most of the airfoil was free of ice.

It should be noted that the biggest advantage of the AC-SDBD plasma actuator is that it can be simultaneously used for flow control as well as ice mitigation using the same plasma actuator device; i.e., the actuators can be used for icing control in icing conditions and flow control in the nonicing environment. Therefore, future efforts will be focused on using the same actuator for both flow control as well as ice-mitigation to quantitatively estimate the flow control effectiveness.

For NS-SDBD plasma actuation, it has great potential in high-speed flow control, and so the combination of NS-SDBD plasma flow control and icing control technology is more attractive. Further investigations should be pursued to study the detailed mechanism for NS-SDBD plasma icing control.

References

[1] Bragg, M. B., Gregorek, G. M., and Lee, J. D., "Airfoil Aerodynamics in Icing Conditions," *Journal of Aircraft*, Vol. 23, No. 1, 1986, pp. 76–81.
https://doi.org/10.2514/3.45269
[2] Thomas, S. K., Cassoni, R. P., and MacArthur, C. D., "Aircraft Anti-Icing and De-Icing Techniques and Modeling," *Journal of Aircraft*, Vol. 33, No. 5, 1996, pp. 841–854.
https://doi.org/10.2514/3.47027
[3] Cao, Y. H., Tan, W. Y., and Wu, Z. L., "Aircraft Icing: An Ongoing Threat to Aviation Safety," *Aerospace Science and Technology*, Vol. 75, April 2018, pp. 353–385.
[4] Whalen, E. A., and Bragg, M. B., "Aircraft Characterization in Icing Using Flight Test Data," *Journal of Aircraft*, Vol. 42, No. 3, 2005, pp. 792–794.
https://doi.org/10.2514/1.11198
[5] Waldman, R. M., and Hu, H., "High-Speed Imaging to Quantify Transient Ice Accretion Process over an Airfoil," *Journal of Aircraft*, Vol. 53, No. 2, 2016, pp. 369–377.
https://doi.org/10.2514/1.C033367
[6] Abbas, A., de Vicente, J., and Valero, E., "Aerodynamic Technologies to Improve Aircraft Performance," *Aerospace Science and Technology*, Vol. 28, No. 1, 2013, pp. 100–132.
https://doi.org/10.1016/j.ast.2012.10.008
[7] Venna, S., Lin, Y. J., and Botura, G., "Piezoelectric Transducer Actuated Leading Edge De-Icing with Simultaneous Shear and Impulse Forces," *Journal of Aircraft*, Vol. 44, No. 2, 2007, pp. 509–515.
https://doi.org/10.2514/1.23996

[8] Nagappan, N., Golubev, V. V., and Habashi, W., "Parametric Analysis of Icing Control Using Synthetic Jet Actuators," AIAA Paper 2013-2453, 2013.
https://doi.org/10.2514/6.2013-2453

[9] Shinkafi, A., and Lawson, C., "Enhanced Method of Conceptual Sizing of Aircraft Electro-Thermal De-Icing System," *International Journal of Mechanical, Aerospace, Industrial and Mechatronics Engineering*, Vol. 8, No. 6, 2014, pp. 1069–1076.

[10] Drury, M. D., Szefi, J. T., and Palacios, J. L., "Full-Scale Testing of a Centrifugally Powered Pneumatic De-Icing System for Helicopter Rotor Blades," *Journal of Aircraft*, Vol. 54, No. 1, 2017, pp. 220–228.
https://doi.org/10.2514/1.C033965

[11] De Pauw, D., and Dolatabadi, A., "Effect of Superhydrophobic Coating on the Anti-Icing and Deicing of an Airfoil," *Journal of Aircraft*, Vol. 54, No. 2, 2017, pp. 490–499.
https://doi.org/10.2514/1.C033828

[12] Liu, Y., Bond, L. J., and Hu, H., "Ultrasonic-Attenuation-Based Technique for Ice Characterization Pertinent to Aircraft Icing Phenomena," *AIAA Journal*, Vol. 55, No. 5, 2017, pp. 1602–1609.
https://doi.org/10.2514/1.J055500

[13] Juuti, P., Haapanen, J., Stenroos, C., Niemelä-Anttonen, H., Harra, J., Koivuluoto, H., Teisala, H., Lahti, J., Tuominen, M., Kuusipalo, J., Vuoristo, P., and Mäkelä, J. M., "Achieving a Slippery, Liquid-Infused Porous Surface with Anti-Icing Properties by Direct Deposition of Flame Synthesized Aerosol Nano-Particles on a Thermally Fragile Substrate," *Applied Physics Letters*, Vol. 110, No. 16, 2017, Paper 161603.
https://doi.org/10.1063/1.4981905

[14] Moreau, E., "Airflow Control by Non-Thermal Plasma Actuators," *Journal of Physics D: Applied Physics*, Vol. 40, No. 3, 2007, pp. 605–636.
https://doi.org/10.1088/0022-3727/40/3/S01

[15] Mertz, B. E., and Corke, T. C., "Single-Dielectric Barrier Discharge Plasma Actuator Modelling and Validation," *Journal of Fluid Mechanics*, Vol. 669, Feb. 2011, pp. 557–583.
https://doi.org/10.1017/S0022112010005203

[16] Wang, J. J., Choi, K. S., Feng, L. H., Jukes, T. N., and Whalley, R. D., "Recent Developments in DBD Plasma Flow Control," *Progress in Aerospace Sciences*, Vol. 62, Oct. 2013, pp. 52–78.
https://doi.org/10.1016/j.paerosci.2013.05.003

[17] Roupassov, D. V., Nikipelov, A. A., Nudnova, M. M., and Starikovskii, A. Y., "Flow Separation Control by Plasma Actuator with Nanosecond Pulsed-Periodic Discharge," *AIAA Journal*, Vol. 47, No. 1, 2009, pp. 168–185.
https://doi.org/10.2514/1.38113

[18] Kelley, C. L., Bowles, P. O., Cooney, J., He, C., Corke, T. C., Osborn, B. A., Silkey, J. S., and Zehnle, J., "Leading-Edge Separation Control Using Alternating Current and Nanosecond Pulse Plasma Actuators," *AIAA Journal*, Vol. 52, No. 9, 2014, pp. 1871–1884.
https://doi.org/10.2514/1.J052708

[19] Zhang, X., Li, H. X., Huang, Y., and Wang, W. B., "Wing Flow Separation Control Using Asymmetrical and Symmetrical Plasma Actuator," *Journal of Aircraft*, Vol. 54, No. 1, 2017, pp. 301–309.
https://doi.org/10.2514/1.C033845

[20] Nishihara, M., Takashima, K., Rich, J. W., and Adamovich, I. V., "Mach 5 Bow Shock Control by a Nanosecond Pulse Surface Dielectric Barrier Discharge," *Physics of Fluid*, Vol. 23, No. 6, 2011, pp. 605–622.
https://doi.org/10.1063/1.3599697

[21] Hong, D., Magnier, P., Bauchire, J. M., Dong, B., and Pouvesle, J. M., "Experimental study of a DBD Surface Discharge for the Active Control of Subsonic Airflow," *Journal of Physics D: Applied Physics*, Vol. 41, No. 15, 2008, Paper 155201.
https://doi.org/10.1088/1361-6463/aa6229

[22] DeJoseph, C., Kimmel, R. L., Hayes, J. R., Menart, J., and Stanfield, S. A., "Rotational and Vibrational Temperature Distributions for a Dielectric Barrier Discharge in Air," *AIAA Journal*, Vol. 47, No. 5, 2009, pp. 1107–1115.
https://doi.org/10.2514/1.37648

[23] Joussot, R., Boucinha, V., Rabat, H., Hong, D., Leroy-Chesneau, A., and Weber-Rozenbaum, R., "Thermal Characterization of a DBD Plasma Actuator: Dielectric Temperature Measurements Using Infrared Thermography," AIAA Paper 2010-5102, 2012.
https://doi.org/10.2514/6.2010-5102

[24] Erfani, R., Zare-Behtash, H., and Kontis, K., "Plasma Actuator: Influence of Dielectric Surface Temperature," *Experimental Thermal and Fluid Science*, Vol. 42, Oct. 2012, pp. 258–264.
https://doi.org/10.1016/j.expthermflusci.2012.04.023

[25] Meng, X., Chen, Z., and Song, K., "AC- and NS-DBD Plasma Flow Control Research," Proceedings of the 2nd NPU-DLR Workshop on Aerodynamics, German Aerospace Center (DLR), German Aerospace Institute, Inst. fur Aerodynamik und Stromungstechnik, DLR-IB 124-2014/5, 1-75, Cologne, Germany, 2014.

[26] Meng, X., Cai, J., Tian, Y., Han, X., Zhang, D., and Hu, H., "Experimental Study of Deicing and Anti-Icing on a Cylinder by DBD Plasma Actuation," AIAA Paper 2016-4019, 2016.
https://doi.org/10.2514/6.2016-4019

[27] Cai, J., Tian, Y., Meng, X., Han, X., Zhang, D., and Hu, H., "An Experimental Study of Icing Control Using DBD Plasma Actuator," *Experiments in Fluids*, Vol. 58, No. 102, 2017, pp. 1–8.
https://doi.org/10.1007/s00348-017-2378-y

[28] Kriegseis, J., Simon, B., and Grundmann, S., "Towards In-Flight Applications? A Review on Dielectric Barrier Discharge-Based Boundary-Layer Control," *Applied Mechanics Reviews*, Vol. 68, No. 2, 2016, Paper 020802.
https://doi.org/10.1115/1.4033570

[29] Zhou, W., Liu, Y., Hu, H., Hu, H., and Meng, X., "Utilization of Thermal Effect Induced by Plasma Generation for Aircraft Icing Mitigation," *AIAA Journal*, Vol. 56, No. 3, 2018, pp. 1097–1104.
https://doi.org/10.2514/1.J056358

[30] Tian, Y., Zhang, Z., Cai, J., Yang, L., and Kang, L., "Experimental Study of an Anti-Icing Method over an Airfoil Based on Pulsed Dielectric Barrier Discharge Plasma," *Chinese Journal of Aeronautics*, Vol. 31, No. 7, 2018, pp. 1449–1460.
https://doi.org/10.1016/j.cja.2018.05.008

[31] Liu, Y., Kolbakir, C., Hu, H. Y., and Hu, H., "A Comparison Study on the Thermal Effects in DBD Plasma Actuation and Electrical Heating for Aircraft Icing Mitigation," *International Journal of Heat and Mass Transfer*, Vol. 124, Sept. 2018, pp. 319–330.
https://doi.org/10.1016/j.ijheatmasstransfer.2018.03.076

[32] Meng, X., Hu, H., Li, C., Abbasi, A. A., Cai, J., and Hu, H., "Mechanism Study of Coupled Aerodynamic and Thermal Effects Using Plasma Actuation for Anti-Icing," *Physics of Fluids*, 31, No. 3, 2019, Paper 037103.
https://doi.org/10.1063/1.5086884

[33] Roth, J. R., "Aerodynamic Flow Acceleration Using Paraelectric and Peristaltic Electrohydrodynamic Effects of a One Atmosphere Uniform Glow Discharge Plasma," *Physics of Plasmas*, Vol. 10, No. 5, 2003, pp. 2117–2126.
https://doi.org/10.1063/1.1564823

[34] Zhang, X., Li, H., Huang, Y., and Wang, W., "Wing Flow Separation Control Using Asymmetrical and Symmetrical Plasma Actuator," *Journal of Aircraft*, Vol. 54, No. 1, 2017, pp. 301–309.
https://doi.org/10.2514/1.C033845

[35] Corke, T. C., Post, M. L., and Orlov, D. M., "Single-Dielectric Barrier Discharge Plasma Enhanced Aerodynamics: Concepts Optimization, and Applications," *Journal of Propulsion and Power*, Vol. 24, No. 5, 2008, pp. 935–945.
https://doi.org/10.2514/1.24430